Magnetic control of *Dictyostelium* aggregation

C. Wilhelm,* C. Rivière, and N. Biais
Laboratoire Matière et Systèmes Complexes, CNRS UMR 7057-Université Paris 7, Paris, France
(Received 27 November 2006; revised manuscript received 22 January 2007; published 6 April 2007)

We report the control of cell migration by external magnetic forces during the early stage of *Dictysostelium discoideum* morphogenesis. Magnetically labeled aggregating cells respond to the presence of a magnetic field created by a thin magnetic tip: forces as low as 30 pN are sufficient to elicit the aggregation of the cells at the extremity of the tip. This induced magnetotaxis is competitive to classical chemotaxis. We therefore underline the interplay between external mechanical forces and morphogenesis. This magnetic assay will open new possibilities in the study of morphogenesis in *Dictyostelium*.

DOI: 10.1103/PhysRevE.75.041906 PACS number(s): 87.18.Ed, 87.17.Jj, 87.15.La, 85.70.−w

For years the morphogenesis of biological entities was thought to be primarily of chemical origin [1]; but explaining development in shaping living communities now requires integration of complex events from genetic regulation to physical mechanisms [2,3]. Going down at the level of a single eukaryotic cell, there is a growing body of experimental evidence reassessing the importance of physical stimuli in cell life. In this way, substrate stiffness governs cell growth and differentiation [4] and many nonchemical signals have been shown to influence the migration of cells [e.g., light (phototaxis [5]), and electrical potential (galvanotaxis [6]), and stiffness (durotaxis [7])]: the well-studied chemotaxis (impact of chemicals on cell migration) is no more the only role-player in directed motion.

Particularly, mechanical forces are key factors to explain the migration of cells because they are mandatory in order to allow any motion. Recently, scores of new methods have emerged to measure the forces exerted by a cell while it is crawling [8–12] or the viscoelastic response of cells to mechanical stresses [13–17]. Altogether those experiments have yielded considerable new insights on cell mechanical properties. However, the impact of external mechanical forces on cell migration, sometimes referred to as mechanotaxis, is scarcely investigated [18–20]. Evolution provides examples of organisms from bacteria to pigeons that use magnetic forces to guide their path (magnetotaxis [21]). In those cases, magnetotaxis is generally due to the presence of a magnetic force sensor in which a small signal is amplified and integrated in a multistep process to lead to the decision of moving along magnetic field lines.

In this paper, we are presenting a well-studied morphogenetic sequence (the aggregation of the social amoeba *Dictyostelium discoideum*) that is thought to be controlled by chemotaxis. We are adding in the possibility to exert external (magnetic) forces on the cells during this morphogenetic process by conferring them magnetic properties. We therefore examine the interplay between chemotaxis and magnetically induced mechanotaxis.

The multicellular organism *Dictyostelium discoideum* is a powerful, accessible, and simple model system for the study of a variety of fundamental cellular processes including chemotaxis, intercellular communication, and morphogenesis [22–24]. In normal food conditions, *Dictyostelium* consists of separate free living cells. Upon starvation, morphogenesis is initiated: cells enter into aggregation streams and collect in the aggregation center to form a mound of cells which transform into a motile slug and finally a fruiting body.

We focus in this paper on the premorphogenesis aggregation period of these social cells: during hours following the removal of food sources, a chemotactic response develops which drives the movement of cells into radial branching structures (streams). Over the last decades, a large amount of information has been accumulated on the nature of this spontaneous mass movement of cells. There is now strong experimental evidence for the essential role of the signaling molecule cAMP (cyclic adenosine monophosphate) in cells aggregation. Extracellular cAMP acts both as a chemoattractant (cells exhibit directional movement towards a source of cAMP and collect at the point source) and as a cell-cell signal relay molecule (cells stimulated by cAMP secrete additional cAMP, generating lines of cells that are held together by end-to-end adhesion) [25].

Thanks to a highly efficient cellular magnetic labeling [26], each cell of the *Dictyostelium* cell population bears a magnetic moment with a mean of $M=(2.2\pm0.9)\times10^{-13}$ A m^2 (2.7×10^6 magnetic nanoparticles per cell). Briefly, the labeling is performed in growth medium (HL5), by incubating for 12 h *Dictyostelium* cells with 8 nm diameter iron oxide anionic magnetic nanoparticles at an extracellular iron concentration [Fe]=100 m*M* (corresponding to about 6×10^{15} nanoparticles/ml). Nanoparticles follow the endocytosis pathway and concentrate inside intracellular preexisting vesicles, endosomes, becoming magnetic [26,27]. The cellular magnetic load is measured using a magnetophoresis assay [28]. Once labeled, cells are starved in phosphate buffer (20 m*M* K2HPO4/KH2PO4, *p*H 6.5) to induce aggregation and allowed to adhere on 3.5 cm diameter Petri dishes, at a cell density of 5×10^6 cells per dish. From that time on, cells' behavior is monitored and recorded with a digital videomicroscopy setup. Cells are either left to evolve on their own (control experiments) or in the presence of a magnetic tip (magnetotactic experiments). We use different tip's sizes and shapes to obtain a wide range of forces. Car-

*Corresponding author. Electronic address: claire.wilhelm@univ-paris-diderot.fr

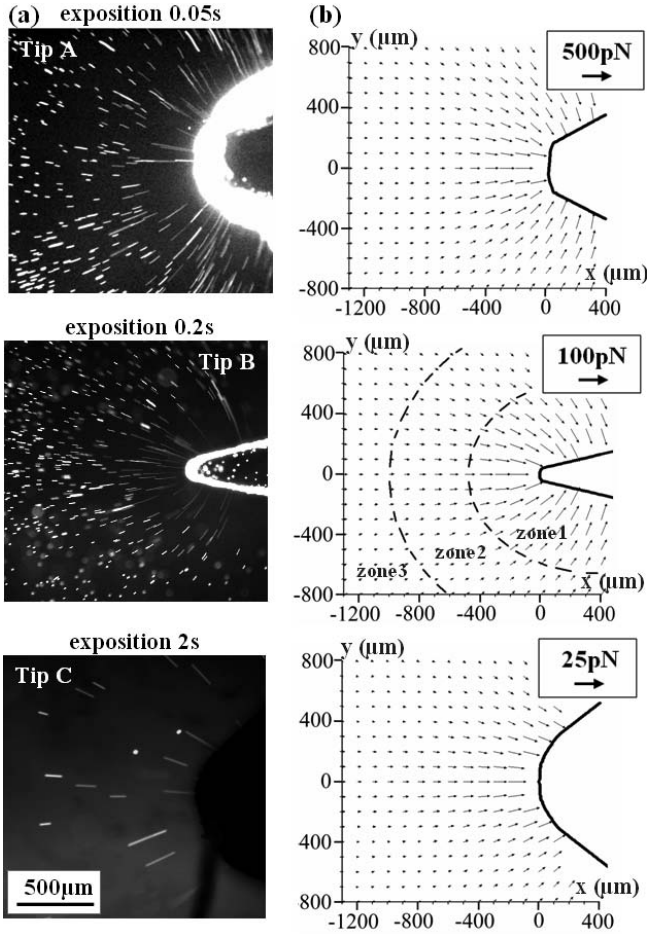

FIG. 1. Magnetic tips calibration. (a) Analysis of the trajectories of magnetic fluorescent beads under the action of magnetic tip A (up–exposition 0.05 s), B (middle–exposition 0.2 s), and C (bottom–exposition 2 s). For each bead, the measure of the velocity directly gives the local magnetic field gradient. (b) The corresponding magnetic forces applied on individual *Dictyostelium* cells were computed from magnetic beads velocities and their cartography is presented in the observation window for the three magnetic tips. Magnetic tips B and C develop magnetic field gradients 4 and 20 times lower than tip A, respectively.

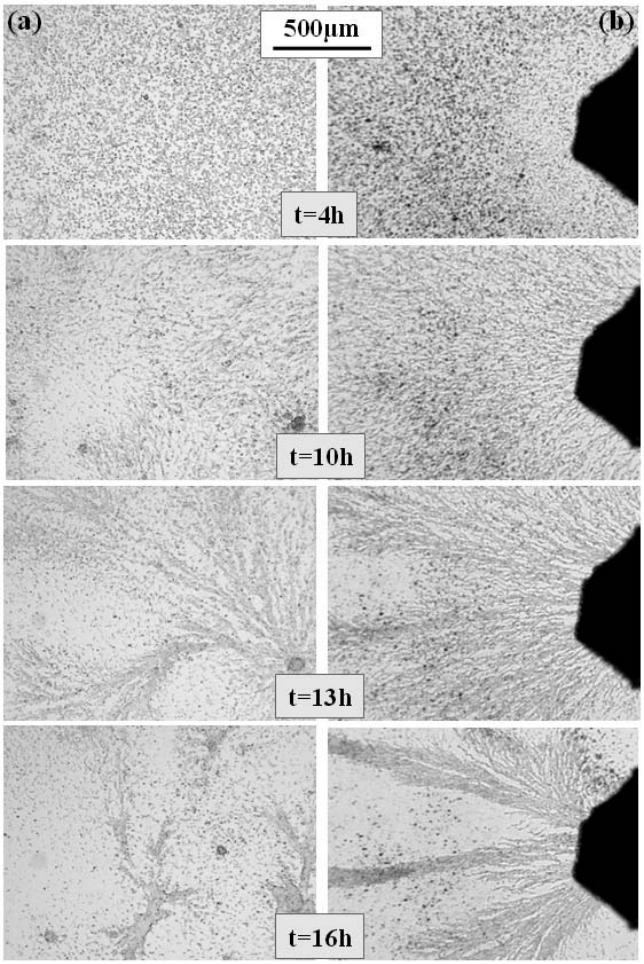

FIG. 2. Aggregation sequence images. Image sequence of aggregation of *Dictyostelium* cells for control conditions (a) and when cells are submitted to a magnetic field gradient (created by tip A) (b). At $t=4$ h, cells are mainly found as individuals for both conditions. Streams of cells are detected from t=10 h. While for control experiments, those streams lines move towards unstable aggregation centers and keep changing directions, they are attracted towards the magnetic tip when submitted to the magnetic field gradient. A video (6000×) is available as electronic supplementary information [40].

tographies of the magnetic forces that those tips would exert on a single magnetically labeled *Dictyostelium* cell are shown in Fig. 1. In order to calibrate the force, we followed the movement of fluorescent magnetic beads in a glycerol-water mixture of known viscosity and thus calculated the map of the magnetic field gradient generated by the tips. Knowing the cells' magnetic moment, we can compute the force exerted by the tip on the cells. The forces range from 1 to 380 pN depending on the tip and on the distance to it.

The typical time course of an experiment is as follows. During the first hours of starvation, cells remain as individuals [Fig. 2(a)—t=4 h] and their migration is not affected by the magnetic forces, even for the closest cells to the tip, where the force is maximal. Indeed, for control conditions (no magnetic tip) as well as under the influence of the magnetic force, the mean square displacement $\langle r^2(t)\rangle$—calculated by computing the Cartesian coordinates of each cell track (during the first 2 h, position measurement every 1 min)—reveals random motion: $\langle r^2(t)\rangle = Dt^{\alpha}$, with exponent α near unity [control conditions: $\alpha=(1.06\pm0.08)$; near tip A: $\alpha=(1.05\pm0.06)$]. Averaged cell velocity calculated with an observation interval of 1 min is not modified [control conditions: $v=(4.1\pm0.9)$ μm/min; near tip A: $v=(4.6\pm0.6)$ μm/min] and the value is in the same range as other reported values for individual *Dictyostelium* cells (e.g., 9 μm/min [29], 4–20 μm/min [30], (5.9 ± 4.5) μm/min [31], and 10 μm/min [32]). This observation is coherent with the strong (few nNs) crawling forces recorded for *Dictyostelium* [33]. Without the triggering of a signal by the external forces, there is little chance that a force about a tenth of the crawling forces can affect the cells migrating behavior. Everything is drastically different as cells start interacting and lining end-to-end [Fig. 2(b)—t=10 h]: the formed streams orient along

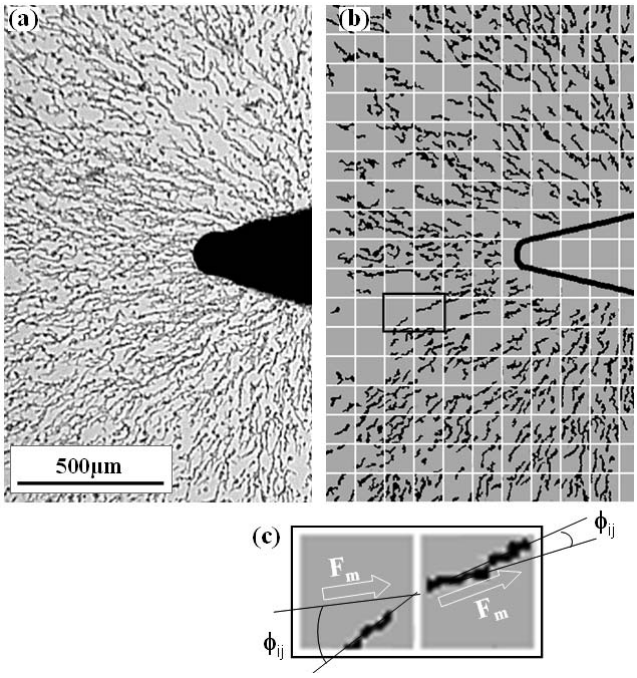

FIG. 3. Image analysis. Every time interval (1 or 10 min), transmission images (a) are binarized to underline stream lines, and are subdivided in 100×100 μm^2 squares (b). For every square [coordinate (i,j), example in (c)], the length of the absolute angle $\phi_{i,j}$ (0°–90°) between the direction of the stream and the magnetic forces is computed.

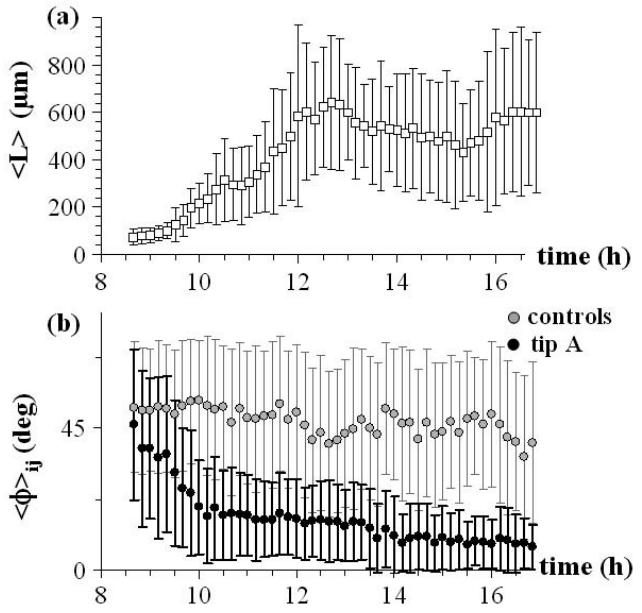

FIG. 4. Data analysis: Onset of collective regime. (a) For each time of aggregation, the spatial average $\langle L\rangle_{ij}$ of the length of the streams is averaged for all experiments (controls and cells submitted to each of the three magnetic tips). Error bars are presented together with the corresponding $\langle L\rangle$ value and represent the deviation from one experiment to the other. As $\langle L\rangle$ reaches approximately 200 μm, we consider that cells have entered the collective aggregative regime. (b) Spatial average $\langle\phi\rangle_{ij}$ of the absolute angle between streams of cells and lines of magnetic forces. Direction of the magnetic field gradient: 0° averaged angle corresponds to all streams oriented in the direction of the magnetic forces, whereas 45° averaged angle shows no preferential direction of the streams. For cells submitted to magnetic tip A (black circles), as the collective regime starts, the angle falls toward 0°, reflecting the alignment of the streams along the magnetic forces, whereas for control cells (white circles), the averaged angle is constant and equals about 45°. Bars represent the standard deviation of the ϕ_{ij} measured angles over the observation window. Therefore for control experiments, where no preferential direction is observed, this deviation is large as the angle is distributed all over the range 0°–90°. In contrast the variation between the $\langle\phi\rangle_{ij}$ obtained for each independent experiment does not exceeds 10% of the mean value (bars not shown for clarity).

the lines of magnetic forces. From this point on, cells react to the magnetic forces. Streams gradually disappear while cells collect in the aggregation center, under the magnetic tip [Fig. 2(b)—t=13–16 h]. This sequence of events is reminiscent of the chemotactic assays using an external cAMP gradient imposed by a micropipette that imposes the position of the aggregation center. In control experiments [Fig. 2(a)] or when the magnetic forces are too low, there is hardly an aggregation center in the field of view and the streams keep changing directions.

In order to gain better insights into the mechanisms at play and a more detailed vision of this magnetotactic effect, we quantify the movement of the streams by performing full image analysis as a function of aggregation time (every 10 min) for three independent experiments with tip A and C, and for three control conditions. The controls are obtained with magnetic cells, but no magnetic tips. As shown in Fig. 3, at each time step, the image is subdivided into a square of 100×100 μm^2. For every square (e.g., coordinates i, j) containing streams, we measure the mean angle $\phi_{i,j}$ (absolute value, from 0° to 90°) between the streams and the line of magnetic forces computed in Fig. 1. To summarize for each time point how closely the streams follow the magnetic forces, we calculate the spatial average of the angle $\langle\phi\rangle_{i,j}$. The closer $\langle\phi\rangle_{i,j}$ is to zero, the more streams of cells follow the lines of magnetic forces. $\langle\phi\rangle_{i,j}=45°$ with large deviation means that streams do not show any preferences for the direction of the magnetic force. The $\langle\phi\rangle_{i,j}$ averaged for tip A and control experiments are presented in Fig. 4(b) together with the length of streams [Fig. 4(a)] averaged on the whole image, for all performed experiments, as a function of the aggregating time. We observe that streams massively orient along the magnetic force when averaged lengths of streams reached about 200 μm, after an aggregating time of 10 h following the beginning of starvation. This period represents a collective magnetotactic regime.

In order to easily compare the influence of magnetotaxis in different conditions, we introduce a single number, the magnetotactic index MI. We calculate the time average over the first 4 h after the onset of the collective regime of the spatial average of the angle $\langle\phi\rangle_{i,j}$, $\langle\phi\rangle_{i,j,t}$. The magnetotactic index is defined as $MI=1-\langle\phi\rangle_{i,j,t}/45$. This number by itself sums up the ability to direct the streams along the lines of magnetic forces. MI=0 means that streams do not show any preferences for the direction of the magnetic force. By con-

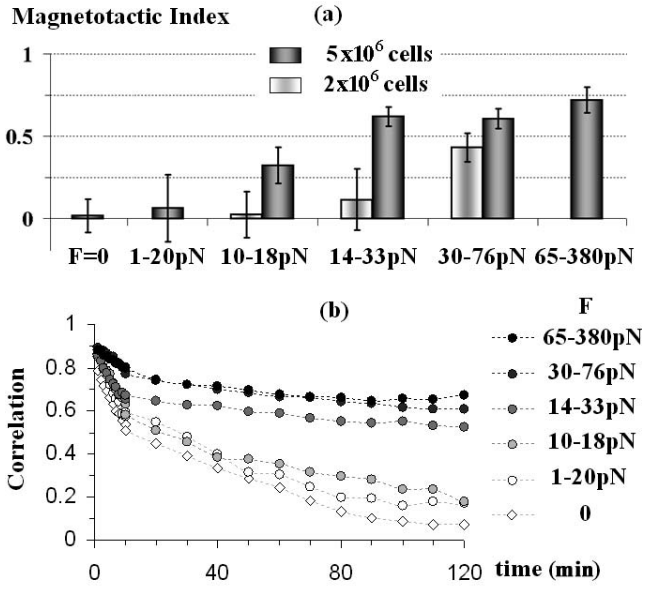

FIG. 5. Data analysis: Magnetotaxis force dependent (a) Magnetotactic index (MI) for all conditions of force tested. As the force reaches the range 14–33 pN we observe the occurrence of magnetotaxis, with an index increasing towards unity (full magnetotaxis). Besides, if we decrease by more than two the usual cell densities used (from 5×10^6 to 2×10^6 cells per dish), magnetotaxis needs a higher force value (range 30–76 pN) to be efficient. (b) The same effect is observed for the correlation function: for controls and low forces experiments, the direction of streams completely decorrelates in about 2 h, whereas, as forces applied reach the range 14–33 pN, the streams keep their direction (along the line of forces) for 2 h (and more). For lower cell densities (2×10^6 cells per dish), we need to be in the range 30–76 pN to observe this correlation (data not shown for clarity).

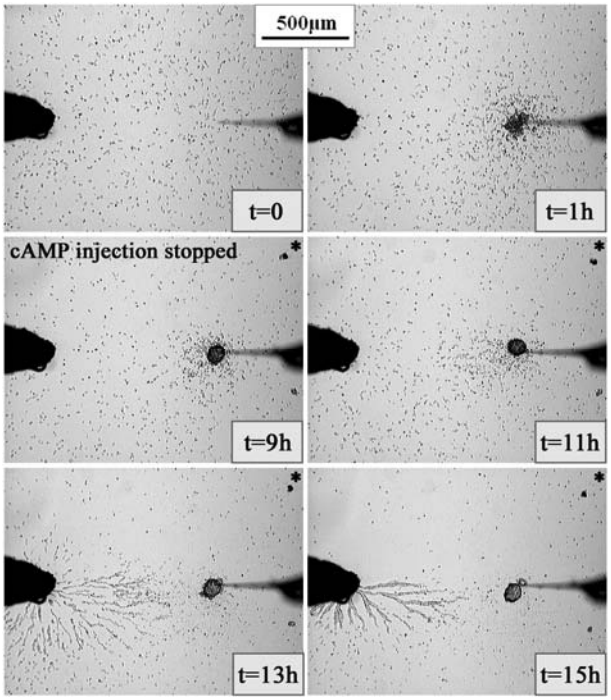

FIG. 6. Magnetotaxis versus chemotaxis. The magnetic tip B is placed in competition with a micropipette which slowly injects a 10 m*M* AMP solution. First, cAMP is injected during a 9 h period, inducing a strong cAMP gradient, and the cells aggregate towards the cAMP tip. Second, cAMP injection is stopped ($t=9$ h). Magnetotaxis is again competitive to chemotaxis and some of the cells are moving back in streams, towards the magnetic tip (streams appear 3 h after stopping cAMP injection). A video (6000 times real time) is available as electronic supplementary information (a star appears when the cAMP injection is stopped).

trast, the increase of MI towards 1 reveals magnetotaxis. As observed in Fig. 4(c), if no magnetotaxis is observed for control conditions (MI=0.02±0.10), when the magnetic tip A is applied (range of forces 65–380 pN), streams tend to move along lines of magnetic forces (MI=0.72±0.05). Besides, experiments with tip C, that is under low magnetic forces (range of forces 1–20 pN), show a low MI (MI=0.06±0.20). Hence we can conclude that a magnetic force of 20 pN is not sufficient to induce magnetotaxis. The use of tip B which exerts forces five times lower than tip A then gives us a more comprehensive view of *Dictyostelium* magnetotaxis. To get a MI equivalent to the MI measured for the entire field of view in the tip A experiments, we need to restrain the spatial averaging to zone 1 or 2 where the force is above 20 pN. Interestingly, there is a residual magnetotatic effect in zone 3, where the force is below 20 pN. An even more intriguing observation is that not only is magnetotaxis dependent on the force, but also on the density of cells. Experiments performed with tip B but seeding only 2×10^6 cells (versus 5×10^6 in all other experiments) show that one needs even greater force than 20 pN to have substantial magnetotaxis (between 30 and 76 pN). In consequence, by using the three magnetic tips, we were able to determine the treshold to impose magnetically induced mechanotaxis against cell chemotaxis: about 20 pN for a high cell density and 35 pN for a lower one. The cells' density has therefore a strong influence on the occurrence of magnetotaxis.

A potential explanation is that there is a synergy in cAMP signaling and magnetotaxis. Upon starvation, after reaching a threshold in cAMP concentration, small streams of magnetic cells are created that would normally either disappear or change direction with time. The presence of the magnetic forces stabilizes and orients those streams. Another way of looking at the persistence in the direction of the streams of cells is to compute the correlation function of the angle, first over time and then over space. To do so, we are first interested in one particular square (e.g., coordinates i, j) and we compute the average over time of the angle between streams and magnetic forces lines separated by $\Delta\tau$: $\Delta\phi_{ij}(\Delta\tau) = \langle\phi_{i,j}(t+\Delta\tau)-\phi_{i,j}(t)\rangle_t$ Then, we calculate the space average $\langle\Delta\phi_{ij}(\Delta\tau)\rangle_{i,j}$ and we define a correlation function $C(\Delta\tau) = 1-\langle\Delta\phi_{ij}(\Delta\tau)\rangle_{i,j}/45$. If the correlation function is around 0, it means the angles are poorly correlated and there is no persistence in the orientation. Increasing the value of $C(\Delta\tau)$ towards unity indicates a correlation and a persistence in the orientation of the angle compared to the magnetic forces. As shown in Fig. 5(b), when no magnetic force is applied (control or low forces conditions), streams stay in the same direction for about 10 min and then lose correlation. By contrast, when the magnetic force reaches the range 14–33 pN

and more, streams follow the same direction for more than 2 h.

Taken together, those observations hint to the hypothesis that the magnetotactic effect that we see is tightly linked to the cAMP chemotaxis. Whether (i) the magnetic forces stabilize nascent aggregates of cells and help them interact or (ii) local high forces nearby the tip are sufficient to trigger a directional motion whose signal can spread globally or (iii) both, there is little doubt that magnetic forces and cAMP work together as a relay of directional signals.

We tried to directly examine the interplay between magnetotaxis and chemotaxis by setting up a competition experiment. If we place face to face, 1 mm apart, tip B and a micropipette that slowly injects a 10 m*M* cAMP solution, the magnetically labeled cells exhibit a strong chemotactic response towards the micropipette (Fig. 6, first two images), creating a dense aggregate of cells at the pipette end. However, when we then stop the flow of cAMP (after 9 h injection), destroying the established cAMP gradient, part of the aggregate packed around the pipette is extracted and streams move towards the magnetic tip: magnetotaxis is restored (Fig. 6, 4 hours and 6 h after stopping the cAMP injection). Hence the global organizing signal of a cAMP gradient prevails on the magnetic influence; but, when there is no such external chemotactic signal, the magnetically induced signal is able to drive the coordinate motion of the cells. This observed competition between chemotaxis and magnetotaxis could be further examined by finely tuning chemotaxis in uniform concentration of cAMP and quantitating magnetotaxis with respect to cAMP.

In conclusion, we have demonstrated that magnetically labeled *Dictyostelium* cells aggregation can be tuned and controlled by the presence of high enough external magnetic forces. The magnetic cells sense the magnetic field generated by a thin magnetic tip and converge at the tip end, at the maximum value of the magnetic field. Beyond a purely chemotactic explanation of the pattern formation seen in *Dictyostelium* [34], there are models taking into account the mechanical properties of the cells and the local mechanical interactions in between the cells [35]. Movement of individual cells is to a large extent constrained to that of the stream. Moreover, consistently with the ability of motile cells to glide against each other as they become integrated into a multicellular structure, intermolecular forces involved in cell-adhesion during the aggregation process have been found to be relatively small compared to other ligand-receptors interactions [36]. Modifications of cell-cell and cell-substrate interactions during stream lines formation may thus also play an important role in this magnetotactic collective migration.

If the exact mechanisms at play in the magnetotactic response we report still need to be investigated, the ability to mechanically control the aggregation of magnetically labeled *Dictyostelium discoideum* appears as a powerful tool to get a more in depth understanding of morphogenetic mechanisms. In particular, it would be interesting to add to the models that describe pattern formation in *Dictyostelium* [37–39] the additional external magnetic force applied to each individual cell.

We thank Irene Tatischeff for providing us the *Dictyostelium* cells and both Florence Gazeau and Jean-Claude Bacri for fruitful discussions and comments.

[1] A. M. Turing, Philos. Trans. R. Soc. London, Ser. B **237**, 37 (1952).
[2] R. Merks and J. Glazier, Physica A **352**, 113 (2005).
[3] E. Farge, Curr. Biol. **13**, 1365 (2003).
[4] P. C. Georges, W. J. Miller, D. F. Meaney, E. S. Sawyer, and P. A. Janmey, Biophys. J. **90**, 3012 (2006).
[5] J. Saranak and K. W. Foster, Nature (London) **387**, 465 (1997).
[6] M. J. Brown and L. M. Loew, J. Cell Biol. **127**, 117 (1994).
[7] C.-M. Lo, H.-B. Wang, M. Dembo, and Y. L. Wang, Biophys. J. **79**, 144 (2000).
[8] T. Oliver, M. Dembo, and K. Jacobson, J. Cell Biol. **145**, 589 (1999).
[9] C. G. Galbraith and M. P. Sheetz, Proc. Natl. Acad. Sci. U.S.A. **94**, 9114 (1997).
[10] J.-P. Rieu, C. Barentin, Y. Maeda, and Y. Sawada, Biophys. J. **89**, 3563 (2005).
[11] S. Usami *et al.*, Biophys. J. **63**, 1663 (1992).
[12] C. Rotsch, K. Jacobson, and M. Radmacher, Proc. Natl. Acad. Sci. U.S.A. **96**, 921 (1999).
[13] A. R. Bausch, W. Moller, and E. Sackmann, Biophys. J. **76**, 573 (1999).
[14] C. Wilhelm, F. Gazeau, and J. C. Bacri, Phys. Rev. E **67**, 061908 (2003).
[15] B. D. Matthews, D. R. Overby, F. J. Alenghat, J. Karavitis, Y. Numaguchi, P. G. Allen, and D. E. Ingber, Biochem. Biophys. Res. Commun. **313**, 758 (2004).
[16] O. Thoumine and A. Ott, J. Chem. Phys. **110**, 2109 (1997).
[17] S. Hu, L. Eberhard, J. Chen, J. Christopher Love, J. P. Butler, J. J. Fredberg, G. M. Whitesides, and N. Wang, Am. J. Physiol.: Cell Physiol. **287**, C1184 (2004).
[18] E. Decave, D. Rieu, J. Dalous, S. Fache, Y. Brechet, B. Fourcade, M. Satre, and F. Bruckert, J. Cell. Sci. **116**, 4331 (2003).
[19] R. Toyoizumi and S. Takeuchi, J. Cell. Sci. **108**, 557 (1995).
[20] C. Riviere, S. Marion, N. Guillen, J. C. Bacri, F. Gazeau, and C. Wilhelm, J. Biomech. **40**, 64 (2007).
[21] R. B. Frankel, Annu. Rev. Biophys. Bioeng. **13**, 85 (1984).
[22] P. J. Van Haastert and P. N. Devreotes, Nat. Rev. Mol. Cell Biol. **5**, 626 (2004).
[23] P. N. Devreotes, Science **245**, 1054 (1989).
[24] C. J. Weijer, Curr. Opin. Genet. Dev. **14**, 392 (2004).
[25] D. Dormann and C. J. Weijer, Curr. Opin. Genet. Dev. **16**, 367 (2006).
[26] C. Wilhelm, F. Gazeau, J. Roger, J. N. Pons, and J. C. Bacri, Langmuir **18**, 8148 (2002).
[27] C. Wilhelm, A. Cebers, J. C. Bacri, and F. Gazeau, Eur. Biophys. J. **32**, 655 (2003).
[28] C. Wilhelm, F. Gazeau, and J. C. Bacri, Eur. Biophys. J. **32**,

655 (2003).
[29] F. Siegert, C. J. Weijer, A. Nomura, and H. Miike, J. Cell. Sci. **107**, 97 (1994).
[30] R. P. Futrelle, J. Traut, and W. G. McKee, J. Cell Biol. **92**, 807 (1982).
[31] E. Shelden and D. A. Knecht, J. Cell. Sci. **108**, 1105 (1995).
[32] R. Escalante, D. Wessels, D. R. Soll, and W. F. Loomis, Mol. Biol. Cell **8**, 1763 (1997).
[33] Y. Fukui, T. Q. P. Uyeda, C. Kitayama, and S. Inoue, Proc. Natl. Acad. Sci. U.S.A. **97**, 10020 (2000).
[34] W.-J. Rappel, A. Nicol, A. Sarkissian, H. Levine, and W. F. Loomis, Phys. Rev. Lett. **83**, 1247 (1999).
[35] E. Palsson and H. G. Othmer, Proc. Natl. Acad. Sci. U.S.A. **97**, 10448 (2000).
[36] M. Benoit, D. Gabriel, G. Gerisch, and H. E. Gaub, Nat. Cell Biol. **2**, 313 (2000).
[37] H. Levine, Chaos **4**, 563 (1994).
[38] C. Van Oss, A. V. Panfilov, P. Hogeweg, F. Siegert, and C. Weijer, J. Theor. Biol. **181**, 203 (1996).
[39] S. Sawai, Y. Maeda, and Y. Sawada, Phys. Rev. Lett. **85**, 2212 (2000).
[40] See EPAPS Document No. E-PLEEE8-75-005704 for (brief description). For more information on EPAPS, see http://www.aip.org/pubservs/epaps.html.